

## Clusters of Galaxies and the Cosmic Web with Square Kilometre Array

Ruta Kale<sup>1,\*</sup> , K. S. Dwarakanath<sup>2</sup>, Dharam Vir Lal<sup>1</sup>,  
Joydeep Bagchi<sup>3</sup>, Surajit Paul<sup>4</sup>, Siddharth Malu<sup>5</sup>, Abhirup Datta<sup>5</sup>,  
Viral Parekh<sup>2</sup>, Prateek Sharma<sup>6</sup> & Mamta Pandey-Pommier<sup>7</sup>

<sup>1</sup>*National Centre for Radio Astrophysics, Tata Institute of Fundamental Research,  
Pune University Campus, Post Bag 3, Ganeshkhind P. O., Pune 411 007, India.*

<sup>2</sup>*Raman Research Institute, C. V. Raman Avenue, Sadashivanagar, Bengaluru 560 080, India.*

<sup>3</sup>*Inter University Centre for Astronomy and Astrophysics (IUCAA), Post Bag 4, Ganeshkhind,  
Pune University Campus, Pune 411 007, India.*

<sup>4</sup>*Department of Physics, Savitribai Phule Pune University, Pune 411 007, India.*

<sup>5</sup>*Indian Institute of Technology Indore, Khandwa Road, Simrol, Indore, 453 552, India.*

<sup>6</sup>*Department of Physics, Indian Institute of Science, Bengaluru 560 012, India.*

<sup>7</sup>*Univ Lyon, Univ Lyon1, Ens de Lyon, CNRS, Centre de Recherche Astrophysique de Lyon  
UMR5574, F- 69230, Saint-Genis-Laval, France.*

\**e-mail: ruta@ncra.tifr.res.in*

Received 19 May 2016; accepted 4 July 2016

**ePublication:** 14 November 2016

**Abstract.** The intra-cluster and inter-galactic media that pervade the large scale structure of the Universe are known to be magnetized at sub-micro Gauss to micro Gauss levels and to contain cosmic rays. The acceleration of cosmic rays and their evolution along with that of magnetic fields in these media is still not well understood. Diffuse radio sources of synchrotron origin associated with the Intra-Cluster Medium (ICM) such as radio halos, relics and mini-halos are direct probes of the underlying mechanisms of cosmic ray acceleration. Observations with radio telescopes such as the Giant Metrewave Radio Telescope, the Very Large Array and the Westerbork Synthesis Radio Telescope have led to the discoveries of about 80 such sources and allowed detailed studies in the frequency range 0.15–1.4 GHz of a few. These studies have revealed scaling relations between the thermal and non-thermal properties of clusters and favour the role of shocks in the formation of radio relics and of turbulent re-acceleration in the formation of radio halos and mini-halos. The radio halos are known to occur in merging clusters and mini-halos are detected in about half of the cool-core clusters. Due to the limitations of current radio telescopes, low mass galaxy clusters and galaxy groups remain unexplored as they are expected to contain much weaker radio sources. Distinguishing between the primary and the

secondary models of cosmic ray acceleration mechanisms requires spectral measurements over a wide range of radio frequencies and with high sensitivity. Simulations have also predicted weak diffuse radio sources associated with filaments connecting galaxy clusters. The Square Kilometre Array (SKA) is a next generation radio telescope that will operate in the frequency range of 0.05–20 GHz with unprecedented sensitivities and resolutions. The expected detection limits of SKA will reveal a few hundred to thousand new radio halos, relics and mini-halos providing the first large and comprehensive samples for their study. The wide frequency coverage along with sensitivity to extended structures will be able to constrain the cosmic ray acceleration mechanisms. The higher frequency (>5 GHz) observations will be able to use the Sunyaev–Zel’dovich effect to probe the ICM pressure in addition to tracers such as lobes of head–tail radio sources. The SKA also opens prospects to detect the ‘off-state’ or the lowest level of radio emission from the ICM predicted by the hadronic models and the turbulent re-acceleration models.

*Key words.* Acceleration of particles—radiation mechanisms: non-thermal—galaxies: clusters: general—large-scale structure of Universe—radio continuum: general.

## 1. Overview

The Square Kilometre Array (SKA) is the next generation radio telescope that will probe the fundamental physics of formation and evolution of galaxies up to large scale structures in the Universe. The SKA has a low-frequency component (SKA1-low) that will be built in Australia and a high frequency component (SKA1-mid) to be built in South Africa. This document gives an overview of the scientific interests of the Continuum Science Working Group members of SKA, India in the field of galaxy clusters and the cosmic web.

## 2. Current SKA1 parameters

A brief description of the currently planned SKA1-mid and the SKA1-low telescopes is provided below. The complete details can be found in the SKA document released in November 2015.<sup>1</sup>

### 2.1 SKA1-mid (0.35–13.6 (20) GHz)

The SKA1-mid telescope is proposed to be a mixed array of 133 15-m SKA1 dishes and 64 13.5-m diameter dishes from the Meer Karoo Array Telescope (MeerKAT). The antennas will be arranged in a moderately compact core with a diameter of

---

<sup>1</sup>SKA-TEL-SKO-0000308\_SKA1\_System\_Baseline\_v2\_DescriptionRev01-part-1-signed.pdf.

Note that the ‘SKA1-SUR’ for which predictions can be found in the articles in AASKA 2014 book has been deferred.

~1 km, a further 2-dimensional array of randomly placed dishes out to ~3 km radius, thinning at the edges. Three spiral arms will extend to a radius of ~80 km from the centre.

The dishes will be capable of operations up to at least 20 GHz, although initially equipped to observe only up to 13.8 GHz for SKA1. MeerKAT dishes are expected to be equipped with a front-end equivalent to SKA Band 2 (0.95–1.76 GHz), a Ultra High Frequency front-end that overlaps with Band 1 (0.3–1 GHz), and an X-band front-end (8–14.5 GHz). Band 2 (0.95–1.76 GHz), 5 (4.6–13.8 GHz) and 1 (0.35–1.05 GHz) will be constructed in priority order as written and the sensitivity at a fiducial frequency of 1.67 GHz is given in Table 1.

### 2.2 SKA1-low (0.05–0.35 GHz)

SKA1-low telescope receptors will consist of an array of ~131,000 log-periodic dual-polarized antenna elements. Many of the antennas will be arranged in a very compact configuration (the ‘core’) with a diameter of ~1 km, the rest of the elements will be arranged in stations, each a few 10 s of metres in diameter. The stations will be distributed over a 40-km radius region lying within Boolardy Station, most likely organized into spiral arms with a high degree of randomization. The antenna array will operate from 50 MHz to ~350 MHz. The antenna elements will be grouped into ~512 stations, whose antennas will be beam-formed to expose a field-of-view of ~20 deg<sup>2</sup>. The expected sensitivity at a fiducial frequency of 0.11 GHz is given in Table 1.

## 3. Introduction: Galaxy clusters, groups and superclusters

The theorized large scale structure of the Universe evolving through initial density fluctuations (e.g. Zel’dovich 1970) has been observed to be a network of filaments and sheets of matter (Spergel *et al.* 2003), interwoven like a ‘web’ (Bond *et al.* 1996) and has been reproduced by cosmological simulations (e.g. Springel *et al.* 2005). Galaxy clusters are the nodes of the ‘web’ having typical masses ~10<sup>14–15</sup> M<sub>⊙</sub> and containing hundreds to thousands of galaxies moving with velocities ~700–1000 km s<sup>-1</sup> (e.g. Girardi *et al.* 1993). Diffuse thermal gas of temperature ~10<sup>7–8</sup> K (a few keV) at cluster cores emits thermal Bremsstrahlung, making clusters extended, soft X-ray emitting sources (e.g. Felten *et al.* 1966; Mitchell & Culhane 1977). This thermal plasma also contains relativistic particles (GeV) and magnetic fields (~0.1–5 μG) and is collectively termed as the Intra-Cluster Medium (ICM). Smaller, less massive (<10<sup>14</sup> M<sub>⊙</sub>) bound systems of galaxies that are found around galaxy

**Table 1.** Sensitivities of SKA1 as of Nov. 2015.

	$\nu^\dagger$ (GHz)	BW (MHz)	rms ( $\mu\text{Jy b}^{-1} \text{h}^{-1/2}$ )	$\theta_b$ (arcsec)
SKA1-mid	1.67	770	0.75	0.25
SKA1-low	0.11	300	3.36	7

<sup>†</sup> Fiducial frequencies as provided by the SKA are used here.

clusters and in-filaments are termed as galaxy groups (e.g. 3C449 and 3C288, Lal *et al.* 2013, 2010). Loosely bound complexes of a number of galaxy clusters and groups are termed as superclusters.

### 3.1 Generation and evolution of cosmic rays

The detectable radio emission from extragalactic sources in and around galaxy clusters is mainly of synchrotron origin. Therefore it is a direct probe of processes that govern the generation and evolution of relativistic particles and magnetic fields in the galaxies themselves and in the diffuse media surrounding them. The variety of radio sources in galaxy clusters can be classified into two broad categories:

- (i) those associated with individual galaxies in the cluster, and
- (ii) those associated with the ICM.

Starbursts (supernovae), Active Galactic Nuclei (AGN) and radio galaxies belong to class (i). These can be compact radio sources or extended sources, but showing obvious association with individual galaxies in the cluster. The class (ii) sources are diffuse extended sources with sizes typically  $\gtrsim 100$  kpc and show no obvious association with individual galaxies. In this work, we will focus mainly on class (ii) sources that are probes of the cosmic ray content and magnetic field in the ICM.

The cosmic rays once produced, will lose energy primarily by synchrotron emission and inverse Compton (IC) scattering of the Cosmic Microwave Background (CMB) photons. The synchrotron losses depend on the energy and magnetic field whereas the IC-losses depend on the energy density of the CMB photons and thus, will scale with redshift as  $(1+z)^4$ . Relativistic protons of energy 1 GeV–1 TeV at cluster cores have radiative lifetimes of several Gyrs but that of the relativistic electrons are about 0.01–0.1 Gyr. The distances over which the cosmic rays can travel within their radiative lifetimes is important to understand the observed source sizes. The dispersal of cosmic rays from their source into the ICM depends on the diffusivity of the ICM. The diffusion time,  $\tau_{\text{diff}}$  taken by cosmic rays to diffuse to distances of Mpc assuming an optimistic spatial diffusion coefficient is several Gyrs (Brunetti & Jones 2014). This implies that cosmic rays once produced will be confined to the cluster and need to be produced *in situ* in the ICM in the case of sources of sizes of 100 s of kpc.

The primary models for the *in situ* generation of Cosmic Ray electrons (CRes) are based on (re-)acceleration of electrons via shocks and turbulence and the secondary models are based on hadronic collisions (see Brunetti & Jones 2014, for a review). The secondary models predict a population of cosmic ray protons (CRp) to accumulate in clusters over its formation that results in relativistic electrons via the collisions of CRps and thermal protons (e.g. Dennison 1980; Blasi & Colafrancesco 1999). An associated gamma ray flux is expected but has not been detected so far; stringent upper limits exist based on the Fermi Gamma Ray Observatory (e.g. Ackermann *et al.* 2010, 2014; Brunetti *et al.* 2012). In the primary models, shocks in the ICM and turbulence are the drivers behind the acceleration of particles and thus are invoked in merging galaxy clusters. Radio observations provide the means to distinguish between the roles of these processes in the generation of synchrotron emission from the ICM.

#### 4. Diffuse synchrotron radio emission from the ICM

Cluster-wide non-thermal radio emission has been a topic of study for nearly half a century since its discovery in the Coma cluster (Large *et al.* 1959; Willson 1970). Over the last few decades, a large number of galaxy clusters were imaged at radio wavelengths (20–200 cm) using a variety of synthesis radio telescopes like the Very Large Array (VLA), the Westerbork Synthesis Radio Telescope (WSRT) and the Giant Metrewave Radio Telescope (GMRT). A large variety in the size, morphology and spectrum of these sources has been found. Based on the properties of the radio sources and the host cluster, the sources have been classified into three<sup>2</sup> main classes (e.g. Feretti *et al.* 2012):

- *Radio halos* – extended sources of sizes  $\sim$ Mpc, nearly co-spatial with X-ray emission from the central regions of clusters.
- *Radio relics* – elongated, filamentary or sometimes arc-like sources of few hundreds to 1–2 Mpc on the longer sides, found at the peripheries of clusters.
- *Radio mini-halos* – extended sources of regular morphologies with sizes  $\sim$ 100–500 kpc, surrounding central elliptical galaxies in cool-core clusters.

Illustrative examples of these sources are shown in Fig. 1. The common components of the ICM which lead to these sources are the relativistic electrons and magnetic fields.

The radio spectra of these sources are typically described by a power-law,  $S_\nu \propto \nu^{-\alpha}$ , where  $S_\nu$  is the flux density at frequency  $\nu$  and  $\alpha$  is the spectral index. The spectral index,  $\alpha$  is related to the injection spectral index,  $\delta$  of the electron energy distribution,  $N(E)dE = N_0 E^{-\delta} dE$  through  $\delta = 2\alpha + 1$  (see textbooks such as Padmanabhan (2000) for details). The spectra originating as a power-law in the case of standard models of particle acceleration can be affected by the effects of overlapping regions of different magnetic fields, age of the electron population, energy losses by other mechanisms such as the IC losses and continuous or intermittent acceleration mechanism. Radio observations over a large range of frequencies are required to study the spectral properties of radio halos, relics and mini-halos and infer the state of the relativistic electron population and magnetic fields. Below we discuss each of these in detail.

The sizes of several hundreds of kiloparsecs in the case of the radio halos imply the role of *in situ* mechanisms of cosmic ray production in the ICM. The primary electron model invokes re-acceleration of electrons from the thermal pool or fossil mildly relativistic electrons via Magneto-HydroDynamic (MHD) turbulence injected by cluster mergers (Petrosian 2001; Brunetti *et al.* 2001; Petrosian & East 2008; Brunetti & Lazarian 2016). The secondary or hadronic model invokes collisions between relativistic protons and thermal protons for producing relativistic electrons in the ICM as secondary products along with associated gamma rays (e.g. Dennison 1980; Blasi & Colafrancesco 1999). Based on the upper limits on the gamma ray fluxes from clusters, simulations show that the relativistic electrons produced via

<sup>2</sup>A fourth class of diffuse radio emission are the so-called ‘radio phoenixes’ which are smaller scale sources that have been proposed to be fading and/or re-accelerated remnants of radio galaxy lobes; these are not discussed in this work.

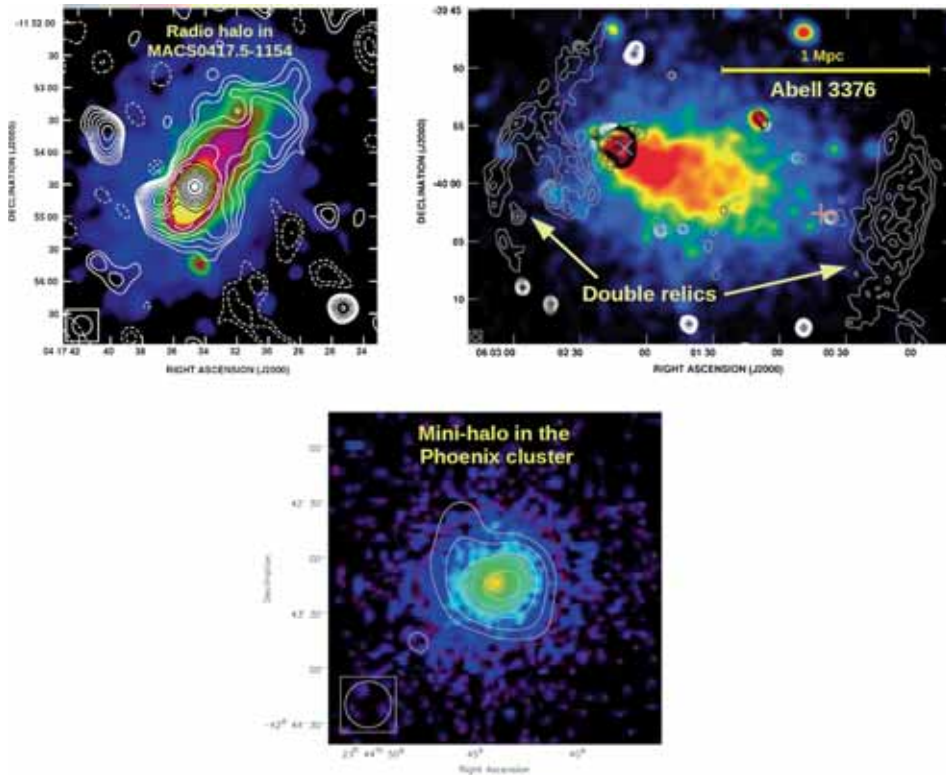


**Figure 1.** Examples of diffuse radio emission in clusters is discussed in this section. The X-ray images are shown in colour scale and radio images in white contours are overlaid. *Top left:* Radio halo in the cluster MACS0417.5-1154. Image adapted from Dwarakanath *et al.* (2011). *Top right:* Double radio relics in the cluster A3376. Image adapted from Kale *et al.* (2012). *Bottom:* Radio mini-halo in the Phoenix cluster. Red contours show the X-ray emission. Image adapted from van Weeren *et al.* (2014a).

hadronic models alone are insufficient to explain the radio halos (e.g. Donnert *et al.* 2013) but can contribute to forming what are called ‘off-state’ radio halos in low mass clusters and relaxed clusters (Brunetti 2011; Brown *et al.* 2011).

The radio emission in relics shows another mode of acceleration of mildly relativistic electrons to ultra relativistic energies via acceleration by shocks. In the large-scale structure there are shocks in the filaments that have Mach numbers of 100 and near-cluster peripheries shocks of Mach numbers of a few (1.5–4) are found (Miniati *et al.* 2000; Kang 2003). Diffusive Shock Acceleration (DSA) has been the proposed model for producing relativistic electrons at the shocks in sources such as the radio relics (e.g. Enßlin *et al.* 1998).

Mini-halos are diffuse sources around the central dominant galaxy in relaxed clusters. The secondary electron model and/or re-acceleration of fossil relativistic electrons by turbulence in the cool core produced due to the infall of sub-clusters inducing sloshing motions have been considered for producing the relativistic electrons responsible for the mini-halos (e.g. Gitti *et al.* 2002; Pfrommer & Enßlin

2004; Fujita *et al.* 2007; Keshet & Loeb 2010; ZuHone *et al.* 2013). A connection between cold-fronts and the mini-halos has also been found (Mazzotta & Giacintucci 2008; Hlavacek-Larrondo *et al.* 2013; Giacintucci *et al.* 2014a, b). The connection between the central galaxy and the mini-halo and the role of external interaction with the cool-core are open questions being addressed using new radio observations and simulations.

#### 4.1 Past studies

**4.1.1 Radio surveys.** The radio observations in the past couple of decades have provided a glimpse of the properties and occurrence rates of the diffuse radio sources in galaxy clusters. The initial discoveries of the radio halos and relics came mainly from the inspection of all-sky radio surveys such as the NRAO VLA Sky Survey (NVSS, Condon *et al.* (1998)). It is a survey at 1.4 GHz carried out using the VLA in D configuration (27 antennas in 1 km<sup>2</sup> area) providing images of the sky with rms sensitivity of 0.45 mJy beam<sup>-1</sup> where beam = 45'' × 45''. A number of radio halos and relics in clusters at redshifts <0.2 were discovered using NVSS and subsequently confirmed with deep follow-up observations (e.g. Giovannini *et al.* 1999; Bagchi *et al.* 2002).

The low surface brightnesses: ~0.2–1 μJy arcsec<sup>-2</sup> at 1.4 GHz of radio halos, relics and mini-halos and their extents of several arcminutes to a degree make them a challenge for imaging with radio telescopes. Aperture synthesis radio telescopes require a combination of short and long baselines to effectively image the extended sources and to separate out the contamination by discrete compact sources. A low-frequency aperture synthesis telescope providing the necessary combination of short and long baselines with sufficient sensitivity to detect faint structures is ideal to carry out tailored surveys of galaxy clusters.

In the past decade, systematic surveys of galaxy clusters at low-radio frequencies (<GHz) have been taken up mainly with the GMRT due to its suitable configuration and sensitivity to extended emission. The GMRT Radio Halo Survey (GRHS) and its extension, the Extended GMRT Radio Halo Survey carried out at 610 MHz, are a systematic deep-radio survey of 64 most X-ray luminous ( $L_{X[0.1-2.4 \text{ keV}]} > 5 \times 10^{44} \text{ erg s}^{-1}$ ) galaxy clusters in the redshift range 0.2–0.4. In the GRHS + EGRHS sample about 22% galaxy clusters contain radio halos, 16% contain mini-halos and 5% contain radio relics (Venturi *et al.* 2007, 2008; Kale *et al.* 2013, 2015). Moreover, the upper limits on the non-detections have showed that there is a bimodality in the clusters such that the detections and non-detections are well separated implying ‘radio bright’ and ‘radio quiet’<sup>3</sup> clusters in the  $P_{1.4 \text{ GHz}} - L_X$  plane. Apart from X-ray flux-limited samples of galaxy clusters that have been explored so far, with the telescopes such as the Planck, the South Pole Telescope and the Atacama Cosmology Telescope that detect clusters using the Sunyaev–Ze’ldovich effect, mass limited samples can now be explored. Radio surveys of complete mass limited samples are ongoing and will provide results in the coming years (Basu 2012; Cuciti *et al.* 2015; Bonafede *et al.* 2015).

<sup>3</sup>This terminology is not connected in any way to the one used in the context of radio galaxies.

4.1.2 *Radio halos and relics.* The observations of radio halos and relics provide the constraints for the particle acceleration mechanisms. The VLA in C and D configurations, the Westerbork Synthesis Radio Telescope (WSRT) and the GMRT have provided the most sensitive measurements of the diffuse radio emission in galaxy clusters in the last two decades. Spectral index distribution across the extents of radio halos is essential to trace the *in situ* acceleration mechanisms and the ageing of the electrons. For this measurement, matched arrays at multiple frequencies are needed and were achieved using a combination of telescopes. The first spectral index maps of radio halos were made with the VLA and the WSRT (e.g. Giovannini *et al.* 1993; Feretti *et al.* 2004). A spectral index study of the radio halo and relic in the cluster A2256 was carried out with a combination of the GMRT at 150 MHz, the WSRT at 350 MHz and the VLA at 1400 MHz (Kale & Dwarakanath 2010). A spectral steepening in the halo at lower frequencies was found in the above observations for the first time and was interpreted in terms of the two epochs of particle acceleration driven by two mergers. Deeper studies with the Karl G. Jansky VLA (JVLA) have further shed light on the spectral properties of the radio relics (Owen *et al.* 2014; Trasatti *et al.* 2015). The follow-up of MASSive Cluster Survey (MACS, Ebeling *et al.* 2010) clusters with the GMRT have led to the discovery of halos, relics and mini-halos in a couple of clusters and a number of other diffuse sources (Dwarakanath *et al.* 2011; Pandey-Pommier *et al.* 2013, 2015, in prep; Parekh *et al.* 2016). The MACS clusters have also been observed at 2–24 GHz with the Australia Telescope Compact Array (ATCA) to study the non-thermal and thermal pressures using diffuse emission and the Sunyaev Zel’dovich Effect (SZE, Malu *et al.* 2016).

The SZE has emerged as a promising probe of discovering new clusters in the past few years. The Planck satellite, the South Pole Telescope and the Atacama Cosmology Telescope have all led to discoveries of new clusters (Planck Collaboration *et al.* 2011, 2014; Reichardt *et al.* 2013; Lindner *et al.* 2015). The first system of radio halo and relic was discovered in a massive new Planck cluster by Bagchi *et al.* (2011) and were followed by discoveries in other clusters (e.g. Giacintucci *et al.* 2013; Bonafede *et al.* 2015). These newly discovered clusters have flatter entropy profiles at the cores and are more likely to be disturbed given the fact that these were missed in the X-ray flux limited catalogues due to their more disturbed morphology. Thus a search for new radio halos and relics in these clusters is on and is furthering the understanding of the role of mass and the dynamical state of the cluster in the generation of radio halos and relics.

Spectral and polarization studies of relics are essential to distinguish between the models for their origin. The prototype of cluster peripheral double relics in the cluster A3376 were discovered and proposed to be the signatures of cluster merger shocks (Bagchi *et al.* 2006). The spectral and polarization studies of the A3376 double radio relics led to the observational evidence of its connection to merger shocks (Kale *et al.* 2012). The low-frequency GMRT observations have been crucial in the discoveries of new radio relics (van Weeren *et al.* 2010, 2011; de Gasperin *et al.* 2015) and radio halos (e.g. Giacintucci *et al.* 2013; van Weeren *et al.* 2014b; Pandey-Pommier *et al.* 2015). The first among the class of ‘ultra-steep spectrum’ radio halos predicted by the turbulent re-acceleration model was found in the cluster A520 using the GMRT (Brunetti *et al.* 2008).

Bagchi *et al.* (2002) discovered the diffuse radio emission associated in a complex system of merging groups of galaxies ZWCl 2341.1+0000 in 1.4 GHz NVSS

survey, and concluded that this emission was the first evidence of cosmic-ray particle acceleration taking place at magnetized cosmic shocks in a highly filamentary environment that is likely in the process of ongoing structure formation. In recent years, more observations of this unusual and highly filamentary merging structure (Fig. 2) and a few other systems have revealed some intriguing details (discussed below) which brought to light unusual aspects of particle acceleration and radio halo and relic formation in elongated, filamentary structures:

- (a) The unusually flat radio spectra of the peripheral double relics ( $\alpha < 0.5$ ) implies high Mach number for the shocks, in contradiction with Mach number estimated from X-ray observations (Bagchi *et al.* 2002; van Weeren *et al.* 2009; Ogreaan *et al.* 2014).
- (b) It is suggested that relics and radio halo in ZWCI 2341.1+0000 highlight the shortcomings or failures of DSA theory in explaining the particle injection spectrum in low mass, less energetic filamentary structures of the cosmic-web (Ogreaan *et al.* 2014). Possibly our understanding of the origin of radio relics is incomplete, and that non-linear effects are required to explain particle acceleration at weak shocks.
- (c) If radio relics result from particle (re-)acceleration at shock fronts, then this shock should span the whole length of the radio relic it traces. Yet in ZWCL 2341.1+000, this expectation is not met, where the SE shock front was found to subtend an arc that is only about a third of the length of the arc subtended by the radio relic; the result was confirmed with a confidence level of  $\sim 90\%$  by Ogreaan *et al.* (2014). Again this result is at odds with the standard DSA theory and needs more investigation with deeper radio observations and modeling.

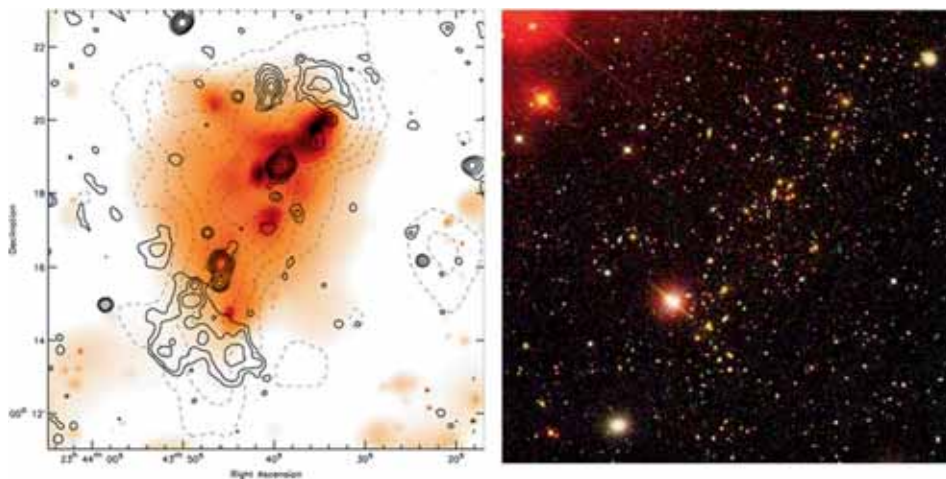


**Figure 2.** Peculiar radio relics found in the filamentary merging cluster ZWCL 2341.1+0000 (Bagchi *et al.* 2002; van Weeren *et al.* 2009). *Left panel:* Radio emission at 610 MHz from GMRT (solid contours), smoothed to a circular beam of  $15''$  to better show the diffuse radio emission. X-ray emission distribution from XMM-Newton observations is shown in the background. Dashed contours show the galaxy iso-density contours from Sloan Digitized Sky Survey. *Right panel:* The SDSS colour image of cluster ZwCl 2341.1+0000 is shown.

The GMRT observations at multiple low frequency bands have been used to distinguish between merger shock related relics and adiabatically compressed lobes of radio galaxies. The adiabatic compression model proposed by Enßlin & Gopal-Krishna (2001) was used to model the spectra of the diffuse emission in A754 and the relics of double radio galaxies (Dwarakanath & Kale 2009; Kale & Dwarakanath 2009). In a multi-wavelength study of radio relics A4038, A1664 and A786, it was found that these are relics not associated with shocks but are adiabatically compressed or fading remnants of radio galaxy lobes (Kale & Dwarakanath 2012). The GMRT low-frequency observations revealed that the radio relic in A4038 is extended to over 100 kpc and what was seen earlier from observations at frequencies 1.4 GHz was only the brightest portion.

**4.1.3 Mini-halos.** Radio mini-halos are diffuse sources, typically of sizes 100–500 kpc that surround the central galaxies in cool-core clusters. The central galaxy always has associated compact source at its centre but is not connected to the surrounding diffuse mini-halo with jets but may have a role in injecting the seed relativistic electrons (e.g. Giacintucci *et al.* 2014b). The secondary electrons due to hadronic collisions may play a role in generating the seed electrons that form the mini-halo but are shown to be insufficient to power the mini-halo (ZuHone *et al.* 2014). It has been proposed that the MHD turbulence in the cool-core, generated via cooling flow or sloshing cores can lead to re-acceleration of relativistic electrons (e.g. Gitti *et al.* 2002; Mazzotta & Giacintucci 2008).

As of now the number count of mini-halos is still limited to about 22 (Giacintucci *et al.* 2014b; Pandey-Pommier *et al.* 2016). About 50% of the cool-core subsample of the clusters in the Extended GMRT Radio Halo Survey were found to host a mini-halo and a scaling between their radio power and the X-ray luminosity was explored (Kale *et al.* 2013). The cooling at the centres and the mini-halos may be connected through scaling relations, but these have not been established due to the lack of statistical samples (e.g. Bravi *et al.* 2016).

Low mass clusters have not been surveyed to search for mini-halos; however there are cases such as the diffuse mini-halo like radio source in the cluster MRC0116+111 which may be remnants of the radio mode activity of the central galaxy (Bagchi *et al.* 2009).

## 4.2 Simulations

Cosmological simulations using computations performed with the grid-based, adaptive mesh refinement hydrodynamical code ENZO show that turbulence in clusters can be sustained on timescales exceeding 1 Gyr (Paul *et al.* 2011). In the same work, it was proposed that the breaking of shocks (seen as high temperature structures in the simulation slices) at inflowing filaments around the cluster can produce notches in the radio relics (Fig. 3). Simulations including magnetic field evolution along with the structure formation and radiative cooling can provide predictions for radio emission from the large-scale structure based on the recipes for production of relativistic electrons (Hoefl & Brüggén 2007; Donnert *et al.* 2013; Vazza & Brüggén 2014; Vazza *et al.* 2015b). It has been shown that a saturation of magnetization can be achieved in a fully turbulent medium and there is near equipartition between the magnetic field and kinetic energy densities (e.g. Subramanian *et al.* 2006; Iapichino

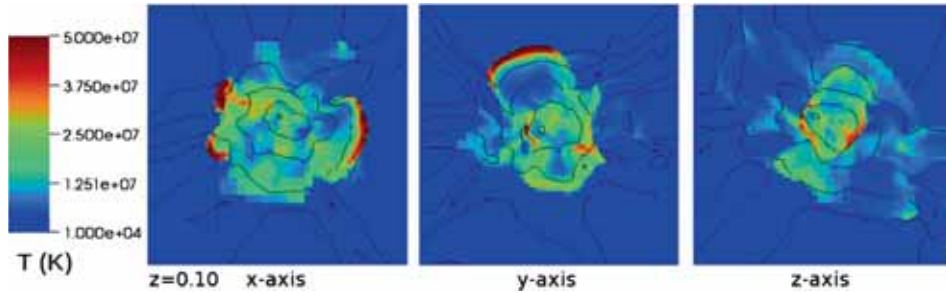


**Figure 3.** Evolution of the shock in temperature in a simulation by Paul *et al.* (2011), as seen from slices in three different planes of the computational volume. The panels refer to  $z = 0.1$  and to slices perpendicular to the x-axis (*left*), y-axis (*central*), and the z-axis (*right*), respectively. Each panel has a size of  $7.7 \times 7.7 \text{ Mpc h}^{-1}$  and is cut along the center-of-mass of the system.

& Brüggén 2012). Magnetic field can be evolved in the simulation using the estimate of turbulence and a scaling between turbulent and magnetic energies. This has been implemented by Paul *et al.* in prep. in the case of Coma and shows agreement with the observed magnetic field profiles (Bonafede *et al.* 2010) based on Faraday rotation of background sources. Radio mini-halos due to electron re-acceleration by minor merger driven turbulence has been simulated by ZuHone *et al.* (2013). Implementation of diffusive shock acceleration and turbulent acceleration to accelerate cosmic rays is being used to predict synchrotron emission that will be observable with the SKA. Predictions by Paul *et al.* (2016) indicate that the estimate of surface brightness at 1.4 GHz with a beam of  $20''$  is about  $10^{-8} \text{ Jy beam}^{-1}$  from the filaments if only turbulent re-acceleration is considered, and in the range  $10^{-6} \text{ Jy beam}^{-1}$  if DSA is also included and denser regions such as groups and cluster outskirts are considered. The uncertainties such as efficiency of turbulent re-acceleration and magnetization in the large-scale structure remain and will be constrained by deeper observations that will be made possible by the SKA.

### 4.3 Prospects for the SKA

In this section, we discuss the numerous possibilities of studying diffuse radio emission from galaxy clusters opened by SKA, thanks to its unprecedented sensitivity.

**4.3.1 Deep continuum and polarization imaging of halos, mini-halos and relics.** Radio halos, relics and mini-halos in general have low surface brightness ( $\sim 1 \mu\text{Jy arcsec}^{-2}$  at 1.4 GHz) and among these, radio halos have the lowest brightness levels. The average surface brightness of the known radio halos at 1.4 GHz is  $\sim 0.25 \mu\text{Jy arcsec}^{-2}$  (inferred using the data in Feretti *et al.* 2012). The SKA1-low will achieve a resolution of  $7'' \times 7''$  at 110 MHz (Table 1). In order to map the extended sources, the images are produced at a lower resolution than the best offered by the telescope configuration. Therefore we assume a canonical resolution of  $10'' \times 10''$  for multi-wavelength observations of diffuse radio sources with the SKA1-low and SKA1-mid and discuss the predictions.

The currently prevalent models of turbulent re-acceleration for radio halos predict that the spectra change from a power-law to an exponential decay beyond a certain critical frequency (Brunetti & Jones 2014). Assuming the critical frequency to be 1.4 GHz, the spectrum corresponding to the mean value of surface brightnesses of known halos is plotted in Fig. 4. The rms confusion at cm wavelengths assuming a Gaussian beam is approximated as (Condon 2002),

$$\left( \frac{\sigma_c}{\text{mJy beam}^{-1}} \right) \approx 0.2 \left( \frac{\nu}{\text{GHz}} \right)^{-0.7} \left( \frac{\theta_b}{\text{arcmin}} \right)^2. \quad (1)$$

The expected rms confusion at the four frequencies of 0.15, 0.6, 1.4 and 5 GHz (Fig. 4) are shown in comparison to the radio halo spectra. It is clear from this figure that most of the known halos can be imaged up to 5 GHz if the cut-off frequency is  $\sim 1.4$  GHz, but, only up to 2 GHz, if the cut-off occurs earlier. The surface brightnesses of diffuse sources are not uniform. The profiles of radio halos show that the central regions are the brightest with a gradual fall towards the edges. With SKA1-low and SKA1-mid, the known radio halos, relics and mini-halos can be imaged to a factor of a few deeper. The profiles of the radio halos in the outskirts of the clusters will provide clues to the underlying cosmic ray and magnetic field profile with implications to the proposed models for the generation of radio halos. It will be possible to reliably map spectral indices over the extent of the radio halos. This will lead to constraints on the *in situ* acceleration mechanisms at work in the cluster. The case

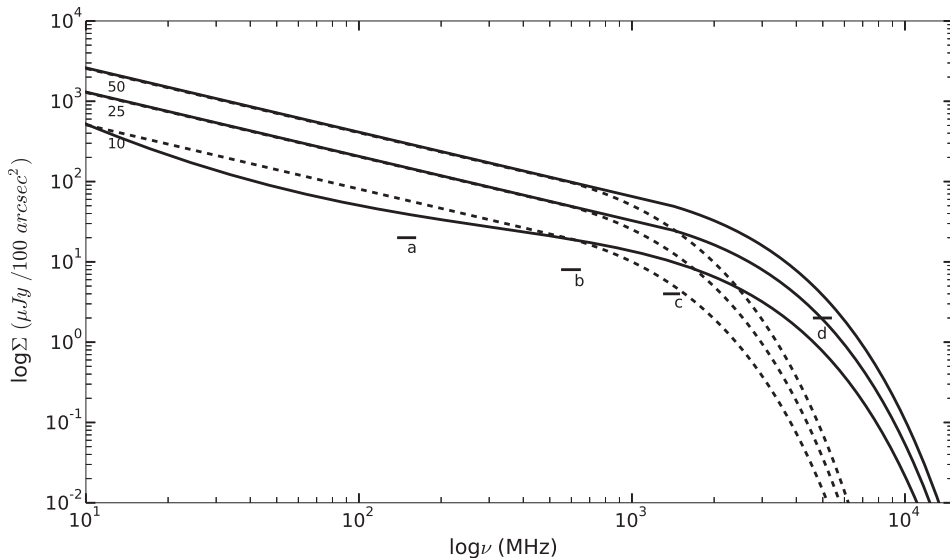


**Figure 4.** Surface brightness of radio halos as a function of frequency. The lines indicate the expected spectra for radio halos that are a combination of a power-law and an exponential decay. The critical frequency where the exponential decay starts is 1.4 GHz (solid lines) and 0.6 GHz (dashed lines), respectively. The three sets of spectra are for three different surface brightness values, 10, 25 and 50  $\mu\text{Jy}/100 \text{ arcsec}^2$  for the halos at 1.4 GHz. The short horizontal lines labelled a, b, c and d indicate the expected confusion limits ( $\mu\text{Jy}/100 \text{ arcsec}^2$ ) at frequencies 0.15, 0.6, 1.4 and 5 GHz, respectively.

of radio halos discussed here is an illustration of the weakest of the diffuse radio sources in clusters. Radio relics and mini-halos being a few times brighter in surface brightness will be imaged in detail leading clues to their origin and evolution.

Furthermore, polarization is a direct probe of the magnetic field in the plane of the sky and complements the line-of-sight magnetic field estimated via Faraday rotation of the plane of polarization of background sources. Through polarization observations, coherence lengths of magnetic field can be inferred and that is used to refine the simulations. Radio halos typically have low polarized emission fraction  $< 5\%$  or so (Feretti *et al.* 2012). Polarization detection was claimed in the radio halo of the cluster A2255 but it is likely due to polarized filament in the periphery of the cluster seen projected on the cluster (Govoni *et al.* 2005; Pizzo *et al.* 2011). Radio mini-halos are at cluster centres and thus depolarization is expected due to the ICM and hence little is known about their polarization properties. Radio relics are known to be polarized up to 10–30%, as expected based on their origin in shock acceleration (see Feretti *et al.* 2012; Brunetti & Jones 2014 for reviews). SKA1-mid sensitivities will allow to probe the polarization properties of these sources to much deeper levels than currently possible and provide important constraints on magnetic fields in clusters of galaxies.

#### 4.3.2 Constraining high frequency spectra of radio halos, relics and mini-halos.

The spectra of radio halos, relics and mini-halos are important to constrain models proposed to explain them. The turbulent re-acceleration model predicts that the spectra will steepen exponentially beyond a break frequency decided by the turbulent energy budget in the cluster (Cassano & Brunetti 2005; Cassano *et al.* 2006). A handful of sources have been imaged at more than three frequency bands below 1 GHz (Feretti *et al.* 2012) and at frequencies higher than a GHz, the spectra are largely unknown. Recently two relics were imaged in the frequency range 0.15–30 GHz using a number of radio telescopes and its spectrum showed departure from the expectations from the DSA model (Stroe *et al.* 2016) but in theoretical works it was argued that DSA can explain it under certain condition of a shock passing through a cloud of fossil population of relativistic electrons (Kang & Ryu 2016). It is important to probe the spectra of these diffuse sources at  $> \text{GHz}$  frequencies to locate the spectral breaks in them and to test the models.

Characterization of galaxy clusters at  $> 10 \text{ GHz}$  is hampered by the presence of the SZE. The distortion of the spectrum of the CMB spectrum due to inverse Compton scattering of the CMB photons by the thermal electrons in the ICM is known as the SZE (Sunyaev & Zeldovich 1972). At frequencies in the range of tens of GHz, the CMB produces a negative signal that can be mixed with the positive radio emission due to radio halos. It is possible to model the signal due to SZE as it has a  $\nu^2$  dependence and to study the radio emission. Studies with ATCA at frequencies 9 and 18 GHz have shown that radio halos (also relics) such as that in the Bullet cluster can be detected, though mixed with the SZE (Malu *et al.* 2010, 2016; Malu & Subrahmanyam 2011).

Observations that match resolutions at high and low frequencies are needed to accurately study the radio halos and the SZE at GHz frequencies. We discuss the expectations for SKA1-mid using Fig. 4. It can be seen that most of the known halos can be imaged up to 5 GHz if the cut-off frequency is  $\sim 1.4 \text{ GHz}$ , but, only up to

2 GHz, if the cut-off occurs at lower frequencies. However the spectra above 2 GHz for the radio halos, relics and mini-halos are largely unknown except in a few cases and presents an obvious niche for new observations.

**4.3.3 Search for new radio halos, relics and mini-halos.** The all-sky continuum surveys and targeted surveys of complete samples of clusters with the SKA will open windows to discover 100 s to 1000 s of new radio halos, relics and mini-halos. The statistical occurrence of the diffuse radio sources is critical to study their origin and evolution in the context of the evolution of the clusters themselves. Current telescopes have allowed a limited number of statistical studies owing to the long observations needed to image with high sensitivity (Venturi *et al.* 2007, 2008; Kale *et al.* 2013, 2015; Cuciti *et al.* 2015; Bonafede *et al.* 2015).

The prospects with the SKA to search for such sources in blind surveys and with targeted observations are promising. From Fig. 4, it is seen that SKA1-low will detect new radio halos as it will reach much better sensitivities than the current instruments. Based on the turbulent acceleration models, it has been predicted that about 2600 new radio halos will be discovered in a survey that can reach rms  $20 \mu\text{Jy beam}^{-1}$  with a beam  $\sim 10''$  at 120 MHz (Cassano *et al.* 2015). From the studies of the known radio halos, it has been inferred that about 58% of the flux density of the radio halo is contained within half its radius (Brunetti *et al.* 2007). A minimum detectable flux density of a radio halo,  $f_{\min}$  can be inferred if it is assumed that a radio halo is detectable when the integrated flux density within half its size gives a signal-to-noise ratio,  $\xi$  (Cassano *et al.* 2015). It means that  $f_{\min}(<0.5\theta_H) \simeq \xi \sqrt{N_b} F_{\text{rms}}$ , where  $N_b$  is the number of independent beams within  $0.5\theta_H$ . It is found that

$$f_{\min} \simeq 1.43 \times 10^{-3} \xi \left( \frac{F_{\text{rms}}}{10 \mu\text{Jy}} \right) \left( \frac{10''}{\theta_b} \right) \left( \frac{\theta_H(z)}{\text{arcsec}} \right). \quad (2)$$

The minimum power of radio halo detectable as a function of redshift for the case of  $\xi = 7.0$  is shown in Fig. 5. The redshifts beyond 0.4 are essentially unexplored and SKA will provide the first glimpse of the properties of radio halos at those redshifts. The ‘off-state’ of clusters which are below the current GMRT upper limits will be detected using the SKA1-low. This is critical to understand the cosmic ray content of galaxy clusters.

## 5. Superclusters and filaments

Binary clusters and systems of multiple interacting clusters can be found in superclusters or as independent systems. Typically such systems may be either in a stage before they fall into each other or could have undergone the merger and are oscillating. In both these cases, it is interesting to study the ICM in and around these clusters to probe the dynamics of diffuse matter and cosmic rays.

Superclusters such as the Shapley SuperCluster (SSC) are among the nearest systems available for study. About 28 clusters were identified within a volume of  $2.5 \times 10^5 \text{ h}^{-3} \text{ Mpc}^3$  – i.e., an over density of more than a factor of ten with respect to the mean density of Abell clusters at similar galactic latitudes (Scaramella *et al.* 1989). SSC is also the richest SC in terms of the presence of X-ray emitting clusters

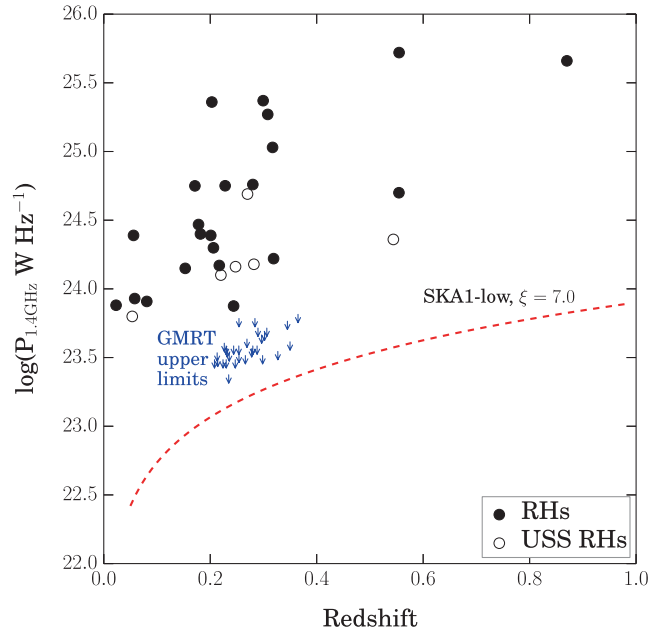


**Figure 5.** The expected detection thresholds for SKA1-low in comparison to the known radio halos. Note that the power at 110 MHz is shown for SKA1-low. If it is scaled to a power at 1.4 GHz, the expected levels are lower by a factor  $(0.11/1.4)^\alpha$ , where  $\alpha$  is the spectral index between 0.11 and 1.4 GHz. The known halos from literature and the GMRT upper limits are from Kale *et al.* (2015).

(Raychaudhury *et al.* 1991). Dedicated studies of this region in optical, radio and X-rays have revealed several sub-structures within this SSC (e.g. Venturi *et al.* 2000 and references therein). Recently, observations of SSC were carried out with the SKA precursor, Murchison Widefield Array (MWA) with the aim of probing diffuse radio emission at cluster and inter-cluster scales (Kale *et al.* 2016).

The SKA1-low opens up the possibility of probing inter-cluster scale radio sources at even better sensitivity than possible with the current MWA. Apart from SSC, other binary clusters and superclusters will be of interest to probe the acceleration of cosmic rays and magnetic fields in these regions. Targets of interest can be filaments between interacting clusters detected by Planck (Planck Collaboration *et al.* 2013).

Apart from the denser structures like the clusters of galaxies and galaxy groups, there are filaments in which a large fraction of the galaxies in the Universe reside. Filaments also contain a large reservoir of inter-galactic medium called the Warm Hot Inter-galactic Medium (WHIM) with temperatures in the range  $10^5$ – $10^7$  K that has been processed by accretion shocks and is extremely difficult to detect in most wavelength bands. Radio bands stand a chance of detecting it if the shocks accelerate electrons. A detection will be able to probe the cosmic rays and magnetic fields in the filaments. Flux densities of  $\sim 0.12 \mu\text{Jy}$  at a redshift of 0.15 at 150 MHz have been predicted assuming that primary electrons are accelerated at cosmological shock waves (Araya-Melo *et al.* 2012). A radio detection of filaments has been predicted in regions where magnetic field is about  $\sim 10$ – $100$  nG (Vazza *et al.* 2015a).

Recent MHD simulations using ENZO have predicted that a non-detection with the SKA can place constraints on the magnetic energy in the WHIM to be less than  $\sim 1\%$  of the thermal energy (Vazza *et al.* 2015b).

Thus although it seems difficult to detect, a strong case exists for detections of filaments surrounding massive clusters. Recently, filaments of temperatures  $\sim 10^7$  K were detected in X-rays around the massive and merging cluster Abell 2744 (Eckert *et al.* 2015). If detected in radio, these can potentially constrain the magnetic field in them.

## 6. Tailed radio galaxies as tracers of inter-galactic weather

### 6.1 Previous studies

‘Tailed’ radio sources (Ryle & Windram 1968) are characterized by a head identified with the optical galaxy and two trails of FRI radio source sweeping back from the head (Miley *et al.* 1972; Jaffe & Perola 1973). These sources are usually found in rich cluster environments, where jets are understood to have been swept back by the deflecting pressure of the dense ICM (Fig. 6). Furthermore, the long tails of these galaxies carry the imprint of relative motion between the non-thermal plasma and the ambient hot gas. Hence, in the parlance of the field, they reflect the weather conditions of ICM and the jet dynamics, which allows us to make quantitative statements about their dynamics and energetics. Two specific examples of the interaction between radio sources and the ICM are Wide-Angle Tailed (WAT) and Narrow-Angle Tailed (NAT) radio sources, where the latter are also addressed as the ‘head–tail’ radio sources.

Recently, a radio study was conducted, using GMRT for a sample of head–tail radio sources, concentrating on 3C129, NGC 1265 and IC 310 (Lal 2009; Lal & Rao 2004). New X-ray observations were proposed for objects which are in poor environments where temperature and abundance variations are likely to be more visible in the X-rays (Rhee *et al.* 1994). When combined with radio data, these multi-waveband

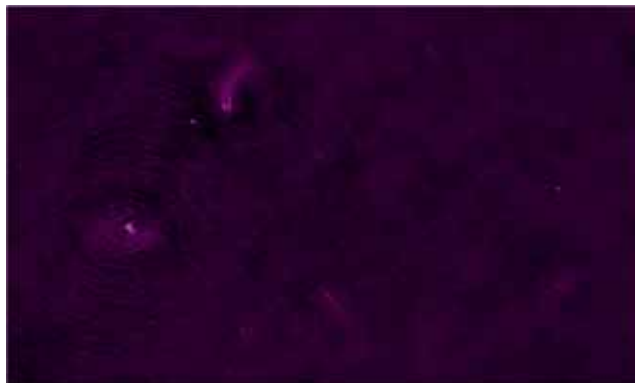


**Figure 6.** Low frequency, full synthesis GMRT image of head–tail sources in Perseus cluster at 240 MHz. Note the presence of a dominant 3C84 radio source and several head–tail radio galaxies, including NGC1265 and IC310. The field is 4 sq. deg, rms noise is  $8.1 \text{ mJy beam}^{-1}$  and the angular resolution is 9 arcsec.

data probe a variety of studies, namely (i) collimation and surface brightness of the jets (Laing & Bridle 2002, 2014), (ii) radio jet–ICM interaction (Perucho *et al.* 2012; Perucho 2012), (iii) infall of tailed radio sources into the cluster, (iv) details of cluster merger (Douglass *et al.* 2011), (v) gas pressure to compare with equipartition pressure, (vi) energy losses, particle acceleration, and (vii) cluster centre ambiguities. The potential of such observations is also to reveal details of cluster mergers such as subsonic/transonic bulk flows, shocks and turbulence. Fortunately, the jets survive the encounter with the ICM, with possible shocks leading to the formation of long tails, that are devoid of the growth of Kelvin–Helmholtz instabilities (Loken *et al.* 1995).

## 6.2 Prospects for the SKA

To illustrate in detail, let us consider two specific science cases related to jets of radio galaxies in cluster environment: (i) is deceleration of jets in these objects caused by internal entrainment or if the mass-load of the jet is external (Perucho 2012; Perucho *et al.* 2011) and (ii) how does the local ICM play a role in shaping NAT and WAT galaxies (Roettiger *et al.* 1996). To answer (i), observationally the transverse velocity profile of the radio jets can give clues to understand which of these two processes is more relevant; if former, no velocity profile across the jet is expected, whereas in the latter case, there would be a velocity profile with slower layers at the jet boundaries (Laing & Bridle 2002). Next to answer (ii), comparisons between the radio morphologies of tailed sources in cluster environments and the distribution of the thermal gas as seen in Chandra and XMM-Newton images, indicate that the thermal gas is almost always asymmetric and aligned towards the direction of the bending (Venkatesan *et al.* 1994), and many a times these clusters are undergoing mergers, resulting in large-scale flows of hot gas owing to the changing gravitational potential (Klamer *et al.* 2004). Therefore tailed radio sources in merging clusters are diagnostics of the ICM weather and of the evolving gravitational potential resulting from the merger as compared to (tailed) radio sources in relaxed clusters. This argument clearly answers the role played by relaxed and merging clusters in shaping WATs and NATs.

A series of tiered surveys with increasing sensitivity, but decreasing in areas are planned to be undertaken with SKA phase-1 (SKA-1). Briefly, the 1–2 GHz band of SKA 1, with 2 arcsec resolution and  $2 \mu\text{Jy beam}^{-1}$  will detect several orders of more number of WAT and NAT radio sources and hence their parent clusters with whom they are associated. Clearly, at this resolution and depth we will not only resolve the radio jet in longitudinal direction, but also in transverse direction and boost our statistical understanding of at least two specific science cases discussed above.

## 6.3 Building statistics using SKA

VLA Faint Images of the Radio Sky at Twenty-cm (FIRST) survey listed  $\sim 384$  WAT and NAT radio sources selected from  $3000 \text{ deg}^2$  of sky. Blanton *et al.* (2001) have confirmed the existence of 40 clusters with redshifts up to  $z \simeq 0.9$ . To compare these, we next try to understand the number of WATs and NATs likely to be detected with SKA surveys. The current deep surveys of smaller parts of the sky such as the  $\sim 4 \text{ deg}^2$  of the ATLAS-CDFS (Australia Large Area Survey of the Chandra Deep

Field–South) field was performed using ATCA at 1.4 GHz (Norris *et al.* 2011) with  $\sim 11$  arcsec resolution and a depth of  $15 \mu\text{Jy beam}^{-1}$ . Additionally, VLA image of the Extended-CDFS, again at 1.4 GHz with  $\sim 2$  arcsec resolution has a depth of  $10 \mu\text{Jy beam}^{-1}$  (Miller *et al.* 2013). Although SKA 1 survey will be similar to this resolution, it will be marginally more sensitive to the VLA–Extended-CDFS (Figure 5 of Dehghan *et al.* 2014; Fig. 1 of Johnston-Hollitt *et al.* 2015a, b). The above surveys detected  $\sim 3000$  radio sources, of which 45 are WAT or NAT radio sources and the rest are extended or (complex) diffuse or ambiguous (Dehghan *et al.* 2011). Extrapolating from these detections, again using (Fig. 1 of Johnston-Hollitt *et al.* (2015a), the SKA level surveys will detect  $\sim 10^6$  WAT and NAT radio sources. The all-sky radio continuum survey using SKA 1 will provide more sensitive data to explore a variety of science goals, including a huge sample,  $\sim 10^6$  clusters of galaxies containing WAT and NAT radio sources. Statistical studies of such large samples of tailed-radio sources will provide insights into both the internal characteristics of astrophysical jets and the surrounding ICM.

## 7. Summary

This chapter highlights the scientific problems in the area of galaxy clusters and the cosmic web that can be effectively addressed using the Square Kilometre Array. The outstanding problems that need to be addressed are:

- (a) the production and sustenance of relativistic particles and magnetic fields that are responsible for the observed diffuse radio emission on cluster-wide scales,
- (b) the relative importance of shocks, turbulent acceleration and hadronic models to the production of cluster-wide radio emission,
- (c) the detailed properties of the intra-cluster medium using cluster radio galaxies as tracers, and
- (d) the faint radio emission arising in structure formation shocks (the cosmic web).

An underlying theme in the observational study of clusters and the cosmic web is the detection of low surface brightness and extended radio emission over a wide range of frequencies such as 0.1–10 GHz. SKA, with its long baselines and good short spacing coverage, will be an ideal instrument to detect these features. It is expected that SKA will reach detection limits that are a factor of 10 to 50 lower compared to those of the existing telescopes. This improved sensitivity is expected to discover an order of magnitude larger number of clusters with faint diffuse radio emission hitherto undetected. These observations from SKA are expected to revolutionize the field of clusters and the cosmic web.

## References

- Ackermann, M. *et al.* 2014, *ApJ*, **787**, 18.  
 Ackermann, M. *et al.* 2010, *ApJ*, **717**, L71.  
 Araya-Melo, P. A., Aragón-Calvo, M. A., Brüggén, M., Hoefl, M. 2012, *MNRAS*, **423**, 2325.  
 Bagchi, J., Enßlin, T. A., Miniati, F., Stalin, C. S., Singh, M., Raychaudhury, S., Humeshkar, N. B. 2002, ArXiv e-prints, 7, 249.  
 Bagchi, J., Durret, F., Neto, G. B. L., Paul, S. 2006, *Science*, **314**, 791.

- Bagchi, J., Jacob, J., Gopal-Krishna Werner, N., Wadnerkar, N., Belapure, J., Kumbharkhane, A. C. 2009, *MNRAS*, **399**, 601.
- Bagchi, J. *et al.* 2011, *ApJ*, **736**, L8.
- Basu, K. 2012, *MNRAS*, **421**, L112.
- Blanton, E. L., Gregg, M. D., Helfand, D. J., Becker, R. H., Leighly, K. M. 2001, *AJ*, **121**, 2915.
- Blasi, P., Colafrancesco, S. 1999, *Astropart. Phys.*, **12**, 169.
- Bonafede, A., Feretti, L., Murgia, M., Govoni, F., Giovannini, G., Dallacasa, D., Dolag, K., Taylor, G. B. 2010, *A&A*, **513**, A30.
- Bonafede, A. *et al.* 2015, *MNRAS*, **454**, 3391.
- Bond, J. R., Kofman, L., Pogosyan, D. 1996, *Nature*, **380**, 603.
- Bravi, L., Gitti, M., Brunetti, G. 2016, *MNRAS*, **455**, L41.
- Brown, S., Emerick, A., Rudnick, L., Brunetti, G. 2011, *ApJ*, **740**, L28.
- Brunetti, G. 2011, *MMSAI*, **82**, 515.
- Brunetti, G., Jones, T. W. 2014, *Int. J. Mod. Phys. D*, **23**, 30007.
- Brunetti, G., Lazarian, A. 2016, *MNRAS*.
- Brunetti, G., Setti, G., Feretti, L., Giovannini, G. 2001, *MNRAS*, **320**, 365.
- Brunetti, G., Venturi, T., Dallacasa, D., Cassano, R., Dolag, K., Giacintucci, S., Setti, G. 2007, *ApJ*, **670**, L5.
- Brunetti, G. *et al.* 2008, *Nature*, **455**, 944.
- Brunetti, G., Blasi, P., Reimer, O., Rudnick, L., Bonafede, A., Brown, S. 2012, *MNRAS*, **426**, 956.
- Cassano, R., Brunetti, G. 2005, *MNRAS*, **357**, 1313.
- Cassano, R., Brunetti, G., Setti, G. 2006, *MNRAS*, **369**, 1577.
- Cassano, R. *et al.* 2015, *Advancing Astrophysics with the Square Kilometre Array (AASKA14)*, **73**.
- Condon, J. J. 2002, in: *Astronomical Society of the Pacific Conference Series*, vol. 278, Single-Dish Radio Astronomy: Techniques and Applications, edited by S. Stanimirovic, D. Altschuler, P. Goldsmith and C. Salter, pp. 155–171.
- Condon, J. J., Cotton, W. D., Greisen, E. W., Yin, Q. F., Perley, R. A., Taylor, G. B., Broderick, J. J. 1998, *AJ*, **115**, 1693.
- Cuciti, V., Cassano, R., Brunetti, G., Dallacasa, D., Kale, R., Etori, S., Venturi, T. 2015, *A&A*, **580**, A97.
- de Gasperin, F., Intema, H. T., van Weeren, R. J., Dawson, W. A., Golovich, N., Wittman, D., Bonafede, A., Brügger, M. 2015, *MNRAS*, **453**, 3483.
- Dehghan, S., Johnston-Hollitt, M., Mao, M., Norris, R. P., Miller, N. A., Huynh, M. 2011, *J. Astrophys. Astr.*, **32**, 491.
- Dehghan, S., Johnston-Hollitt, M., Franzen, T. M. O., Norris, R. P., Miller, N. A. 2014, *AJ*, **148**, 75.
- Dennison, B. 1980, *ApJ*, **239**, L93.
- Donnert, J., Dolag, K., Brunetti, G., Cassano, R. 2013, *MNRAS*, **429**, 3564.
- Douglass, E. M., Blanton, E. L., Clarke, T. E., Randall, S. W., Wing, J. D. 2011, *ApJ*, **743**, 199.
- Dwarakanath, K. S., Kale, R. 2009, *ApJ*, **698**, L163.
- Dwarakanath, K. S., Malu, S., Kale, R. 2011, *J. Astrophys. Astr.*, **32**, 529.
- Ebeling, H., Edge, A. C., Mantz, A., Barrett, E., Henry, J. P., Ma, C. J., van Speybroeck, L. 2010, *MNRAS*, **407**, 83.
- Eckert, D. *et al.* 2015, *Nature*, **528**, 105.
- Enßlin, T. A., Gopal-Krishna 2001, *A&A*, **366**, 26.
- Enßlin, T. A., Biermann, P. L., Klein, U., Kohle, S. 1998, *A&A*, **332**, 395.
- Felten, J. E., Gould, R. J., Stein, W. A., Woolf, N. J. 1966, *ApJ*, **146**, 955.
- Feretti, L., Orrù, E., Brunetti, G., Giovannini, G., Kassim, N., Setti, G. 2004, *A&A*, **423**, 111.
- Feretti, L., Giovannini, G., Govoni, F., Murgia, M. 2012, *A&A*, **543**, 54.

- Fujita, Y., Kohri, K., Yamazaki, R., Kino, M. 2007, *ApJ*, **663**, L61.
- Giacintucci, S., Kale, R., Wik, D. R., Venturi, T., Markevitch, M. 2013, *ApJ*, **766**, 18.
- Giacintucci, S., Markevitch, M., Brunetti, G., Zuhone, J. A., Venturi, T., Mazzotta, P., Bourdin, H. 2014a, *ApJ*, **795**, 73.
- Giacintucci, S., Markevitch, M., Venturi, T., Clarke, T. E., Cassano, R., Mazzotta, P. 2014b, *ApJ*, **781**, 9.
- Giovannini, G., Feretti, L., Venturi, T., Kim, K.-T., Kronberg, P. P. 1993, *ApJ*, **406**, 399.
- Giovannini, G., Tordi, M., Feretti, L. 1999, *New Astr. Rev.*, **4**, 141.
- Girardi, M., Biviano, A., Giuricin, G., Mardirossian, F., Mezzetti, M. 1993, *ApJ*, **404**, 38.
- Gitti, M., Brunetti, G., Setti, G. 2002, *A&A*, **386**, 456.
- Govoni, F., Murgia, M., Feretti, L., Giovannini, G., Dallacasa, D., Taylor, G. B. 2005, *A&A*, **430**, L5.
- Hlavacek-Larrondo, J. *et al.* 2013, ArXiv e-prints.
- Hoft, M., Brüggén, M. 2007, *MNRAS*, **375**, 77.
- Iapichino, L., Brüggén, M. 2012, *MNRAS*, **423**, 2781.
- Jaffe, W. J., Perola, G. C. 1973, *A&A*, **26**, 423.
- Johnston-Hollitt, M., Dehghan, S., Pratley, L. 2015a, *Advancing Astrophysics with the Square Kilometre Array (ASKA14)*, 101.
- Johnston-Hollitt, M., Dehghan, S., Pratley, L. 2015b, in: *IAU Symposium*, vol. 313, *Extragalactic Jets from Every Angle*, edited by F. Massaro, C. C. Cheung, E. Lopez and A. Siemiginowska, pp. 321–326.
- Kale, R., Dwarakanath, K. S. 2009, *ApJ*, **699**, 1883.
- Kale, R., Dwarakanath, K. S. 2010, *ApJ*, **718**, 939.
- Kale, R., Dwarakanath, K. S. 2012, *ApJ*, **744**, 46.
- Kale, R., Dwarakanath, K. S., Bagchi, J., Paul, S. 2012, *MNRAS*, **426**, 1204.
- Kale, R., Venturi, T., Giacintucci, S., Dallacasa, D., Cassano, R., Brunetti, G., Macario, G., Athreya, R. 2013, *A&A*, **557**, A99.
- Kale, R. *et al.* 2015, ArXiv e-prints.
- Kale, R. *et al.* 2016, in preparation.
- Kang, H. 2003, *J. Korean Astron. Soc.*, **36**, 111.
- Kang, H., Ryu, D. 2016, ArXiv e-prints.
- Keshet, U., Loeb, A. 2010, *ApJ*, **722**, 737.
- Klamer, I., Subrahmanyan, R., Hunstead, R. W. 2004, *MNRAS*, **351**, 101.
- Laing, R. A., Bridle, A. H. 2002, *MNRAS*, **336**, 328.
- Laing, R. A., Bridle, A. H. 2014, *MNRAS*, **437**, 3405.
- Lal, D. V. 2009, in: *Astronomical Society of the Pacific Conference Series*, vol. 407, *The Low-Frequency Radio Universe*, edited by D. J. Saikia, D. A. Green, Y. Gupta and T. Venturi, p. 157.
- Lal, D. V., Rao, A. P. 2004, *A&A*, **420**, 491.
- Lal, D. V. *et al.* 2010, *ApJ*, **722**, 1735.
- Lal, D. V. *et al.* 2013, *ApJ*, **764**, 83.
- Large, M. I., Mathewson, D. S., Haslam, C. G. T. 1959, *Nature*, **183**, 1663.
- Lindner, R. R. *et al.* 2015, *ApJ*, **803**, 79.
- Loken, C., Roettiger, K., Burns, J. O., Norman, M. 1995, *ApJ*, **445**, 80.
- Malu, S. S., Subrahmanyan, R. 2011, *J. Astrophys. Astr.*, **32**, 541.
- Malu, S. S., Subrahmanyan, R., Wieringa, M., Narasimha, D. 2010, ArXiv e-prints.
- Malu, S., Datta, A., Sandhu, P. 2016, ArXiv e-prints, in preparation.
- Mazzotta, P., Giacintucci, S. 2008, *ApJ*, **675**, L9.
- Miley, G. K., Perola, G. C., van der Kruit, P. C., van der Laan, H. 1972, *Nature*, **237**, 269.
- Miller, N. A. *et al.* 2013, *ApJS*, **205**, 13.
- Miniati, F., Ryu, D., Kang, H., Jones, T. W., Cen, R., Ostriker, J. P. 2000, *ApJ*, **542**, 608.
- Mitchell, R. J., Culhane, J. L. 1977, *MNRAS*, **178**, 75P.

- Norris, R. P. *et al.* 2011, *PASA*, **28**, 215.
- Ogrean, G. A., Brüggen, M., van Weeren, R. J., Burgmeier, A., Simionescu, A. 2014, *MNRAS*, **443**, 2463.
- Owen, F. N., Rudnick, L., Eilek, J., Rau, U., Bhatnagar, S., Kogan, L. 2014, *ApJ*, **794**, 24.
- Padmanabhan, T. 2000, *Theoretical Astrophysics – Volume I, Astrophysical Processes*, p. 622.
- Pandey-Pommier, M., Richard, J., Combes, F., Dwarakanath, K. S., Guiderdoni, B., Ferrari, C., Sirothia, S., Narasimha, D. 2013, *A&A*, **557**, A117.
- Pandey-Pommier, M. *et al.* 2015, in: *SF2A-2015: Proceedings of the Annual meeting of the French Society of Astronomy and Astrophysics*, edited by F. Martins, S. Boissier, V. Buat, L. Cambrésy and P. Petit, pp. 247–252.
- Pandey-Pommier, M. *et al.* 2016, in preparation.
- Parekh, M., Dwarakanath, K. S., Kale, R., Intema, H. 2016, ArXiv e-prints, 1608.02796.
- Paul, S., Iapichino, L., Miniati, F., Bagchi, J., Mannheim, K. 2011, *ApJ*, **726**, 17.
- Paul, S. *et al.* 2016, in preparation.
- Perucho, M. 2012, *Int. J. Mod. Phys. Conference Series*, **8**, 241.
- Perucho, M., Quilis, V., Martí, J.-M. 2011, *ApJ*, **743**, 42.
- Perucho, M., Quilis, V., Martí, J.-M. 2012, in: *Astronomical Society of the Pacific Conference Series*, vol. 459, Numerical Modeling of Space Plasma Slows (ASTRONUM 2011), edited by N. V. Pogorelov, J. A. Font, E. Audit and G. P. Zank, p. 155.
- Petrosian, V. 2001, *ApJ*, **557**, 560.
- Petrosian, V., East, W. E. 2008, *ApJ*, **682**, 175.
- Pfrommer, C., Enßlin, T. A. 2004, *A&A*, **413**, 17.
- Pizzo, R. F., de Bruyn, A. G., Bernardi, G., Brentjens, M. A. 2011, *A&A*, **525**, A104.
- Planck Collaboration *et al.* 2011, *A&A*, **536**, A8.
- Planck Collaboration *et al.* 2013, *A&A*, **550**, A134.
- Planck Collaboration *et al.* 2014, *A&A*, **571**, A29.
- Raychaudhury, S., Fabian, A. C., Edge, A. C., Jones, C., Forman, W. 1991, *MNRAS*, **248**, 101.
- Reichardt, C. L. *et al.* 2013, *ApJ*, **763**, 127.
- Rhee, G., Burns, J. O., Kowalski, M. P. 1994, *AJ*, **108**, 1137.
- Roettiger, K., Burns, J. O., Loken, C. 1996, *ApJ*, **473**, 651.
- Ryle, M., Windram, M. D. 1968, *MNRAS*, **138**, 1.
- Scaramella, R., Baiesi-Pillastrini, G., Chincarini, G., Vettolani, G., Zamorani, G. 1989, *Nature*, **338**, 562.
- Spergel, D. N. *et al.* 2003, *ApJS*, **148**, 175.
- Springel, V. *et al.* 2005, *Nature*, **435**, 629.
- Stroe, A. *et al.* 2016, *MNRAS*, **455**, 2402.
- Subramanian, K., Shukurov, A., Haugen, N. E. L. 2006, *MNRAS*, **366**, 1437.
- Sunyaev, R. A., Zeldovich, Y. B. 1972, *Comments on Astrophysics and Space Physics*, **4**, 173.
- Trasatti, M., Akamatsu, H., Lovisari, L., Klein, U., Bonafede, A., Brüggen, M., Dallacasa, D., Clarke, T. 2015, *A&A*, **575**, A45.
- van Weeren, R. J. *et al.* 2009, *A&A*, **506**, 1083.
- van Weeren, R. J., Röttgering, H. J. A., Brüggen, M., Hoeft, M. 2010, *Science*, **330**, 347.
- van Weeren, R. J., Brüggen, M., Röttgering, H. J. A., Hoeft, M., Nuza, S. E., Intema, H. T. 2011, *A&A*, **533**, A35.
- van Weeren, R. J. *et al.* 2014a, *ApJ*, **786**, L17.
- van Weeren, R. J. *et al.* 2014b, *ApJ*, **781**, L32.
- Vazza, F., Brüggen, M. 2014, *MNRAS*, **437**, 2291.
- Vazza, F., Ferrari, C., Bonafede, A., Brüggen, M., Gheller, C., Braun, R., Brown, S. 2015a, *Advancing Astrophysics with the Square Kilometre Array (AASKA14)*, 97.
- Vazza, F., Ferrari, C., Brüggen, M., Bonafede, A., Gheller, C., Wang, P. 2015b, *A&A*, **580**, A119.
- Venkatesan, T. C. A., Batuski, D. J., Hanisch, R. J., Burns, J. O. 1994, *ApJ*, **436**, 67.
- Venturi, T., Bardelli, S., Morganti, R., Hunstead, R. W. 2000, *MNRAS*, **314**, 594.

- Venturi, T., Giacintucci, S., Brunetti, G., Cassano, R., Bardelli, S., Dallacasa, D., Setti, G. 2007, *A&A*, **463**, 937.
- Venturi, T., Giacintucci, S., Dallacasa, D., Cassano, R., Brunetti, G., Bardelli, S., Setti, G. 2008, *A&A*, **484**, 327.
- Willson, M. A. G. 1970, *MNRAS*, **151**, 1.
- Zel'dovich, Y. B. 1970, *A&A*, **5**, 84.
- ZuHone, J. A., Markevitch, M., Brunetti, G., Giacintucci, S. 2013, *ApJ*, **762**, 78.
- ZuHone, J., Brunetti, G., Giacintucci, S., Markevitch, M. 2014, ArXiv e-prints.